Visible light selective photocatalytic conversion of glucose by TiO_2

Luigi Da Vià, Carlo Recchi, Edgar O. Gonzalez-Yañez, Thomas E. Davies, Jose A. Lopez-Sanchez *

Stephenson Institute for Renewable Energy, Chemistry Department, The University of Liverpool, Crown Street, Liverpool L69 7ZD, UK

ABSTRACT

The visible-light mediated selective photo-oxidation of glucose using unmodified TiO_2 as a catalyst is reported for the first time. The effect of the catalyst to substrate ratio, lamp power and TiO_2 crystalline phases on the conversion and product distribution under both visible and UVA light is explored. Higher conversions were obtained under UVA light but as a result of substantial mineralization through an unselective pathway. Optimization of the reaction conditions resulted in 42% glucose conversion under visible light with 7% selectivity to gluconic acid and 93% selectivity to other partial oxidation products with the total suppression of a mineralization pathway to CO_2. It is also shown that selective glucose conversion can occur under natural sunlight light after 7 h exposure. In this systematic study, we prove that it is indeed possible to use TiO_2 as a photocatalyst to upgrade biomass derivatives selectively by tailoring the reaction conditions. Most importantly, we find the ligand-to-metal charge-transfer effect as a result of glucose adsorption to the surface of TiO_2 determinant in the photo-activity observed under visible light irradiation. Knowledge of this effect along with the careful control of reaction conditions means that the selective photo-catalytic conversion of other biomass derived carbohydrates under visible light is a viable route to higher value chemicals.

© 2016 The Author(s). Published by Elsevier B.V. This is an open access article under the CC BY license (http://creativecommons.org/licenses/by/4.0/).

1. Introduction

The conventional selective oxidation of glucose to gluconic, glucaric or even glycolic acid has been studied extensively using enzymes and heterogeneous catalysts comprising supported metal nanoparticles [1–8]. The application of photocatalysis in the upgrading of biomass, particularly glucose, is receiving increasing attention. There are a number of studies on the photocatalytic reforming of glucose for hydrogen production, in these cases, glucose is used as a sacrificial electron donor and is degraded in the process [9–11]. It has been shown that "biohydrogen" can be successfully generated using TiO_2 supported Pt and Pd photocatalysts allowing simultaneous water purification and energy production [12]. In only a few cases have the products of glucose oxidation been identified or highlighted as valuable side products of water splitting [13]. Recently, glucose oxidation products were identifed as byproducts when glucose was used as a sacrical agent for the *in situ* reduction of organic compounds using the hydrogen produced from water splitting [14,15]. The recent excellent work by Colmenares [16,17] Palmisano [13,18] and Chong [19] deserves to be mentioned

in particular. They reported that the partly selective photocatalytic oxidation of glucose to aldoses such as arabinose, erythrose and glyceraldehyde can be carried out under UV light for a number of photocatalytic systems [17–21] in agreement with observations in our group. However, the ultimate goal for photocatalysis is the development of a catalytic system that can ultimately work within the solar biorefinery concept using sunlight as the energy source. For this, it is fundamental that we develop photocatalytic systems that are active under visible light. This is why most attention is now directed at the modification of TiO_2 by adding a second component to confer visible light activity. However, it would be ideal to perform these transformations using just TiO_2 and visible light. Many photocatalytic processes are associated with unselective or total mineralization reactions aimed at the purification of water and gas streams through the abatement of organic pollutants and contaminants [22–24]. In these applications, TiO_2-based materials show great potential as they are generally chemically stable, non-toxic and have high reactivity. However, TiO_2 is not photoactive under visible light and hence is understandably disregarded for visible-light-driven selective photocatalysis. When considering photocatalyst candidates, we are typically concerned with the mobility and the production rate of the active radical species, but the interaction between the substrate and the catalyst surface is also of fundamental importance and offers new unforeseen opportunities. In fact, the

formation of a complex between TiO_2-glucose was recently identified as being responsible for the activity under visible light of TiO_2 powders for the reduction of Cr (VI) to Cr (III) in solution. The presence of a ligand-to-metal-charge-transfer complex (LMCT) allowed electrons to be injected directly on the conduction band of TiO_2 thus making them available to react [25]. Given these results, we decided to exploit this recent observation to drive the photo-activity of TiO_2 in the photo-conversion of glucose itself, with glucose acting as the reactant and co-catalyst via the formation of the LMCT system. In this work, we report for the first time the activity of TiO_2 for the conversion of glucose under visible light and study the effect of varying the light source, TiO_2 phase, and reaction conditions. The beneficial effect of using visible light on the product distribution, as compared to UVA light, is particularly noteworthy.

2. Experimental

2.1. Materials

The following reagents were used: Titanium (IV) oxide Aeroxide P25 (Acros Organics), titanium (IV) oxide anatase 99.8% (Sigma-Aldrich), titanium (IV) oxide rutile 99.99% (Sigma-Aldrich), acetonitrile (MeCN) HPLC grade 99.9% (Fisher Chemical). HPLC calibration standards: D-(+)-glucose ≥99.5% (GC), D-gluconic acid sodium salt >99%, D-(−)-arabinose ≥98%, D-(+)-glyceraldehyde ≥98%, D-(−)-erythrose ≥75%, formic acid ≥95% were all purchased from Sigma-Aldrich and used without further purification.

2.2. Catalyst preparation

The different TiO_2 phases were dried under vacuum at 100 °C prior to reaction, and the Degussa P25 was heat treated under static air at 500 and 600 °C to increase the rutile to anatase ratio. After heat treatment, the catalysts were ground and stored in a desiccator until further use.

2.3. Catalyst characterization

The solid UV–Vis analysis of the catalysts was performed using a UV-2550 Shimadzu spectrophotometer equipped with an ISR-2200 integrating sphere (Shimadzu Corp, JP) in the range 200–800 nm with a 1 nm sampling interval and a 5 nm slit using $BaSO_4$ as reference. The reflectance data were used to calculate the Kubelka-Munk function using the absolute reflectance ($R\infty$) to evaluate the bandgap of the solid samples.

X-ray diffraction (XRD) patterns were recorded using in transmission mode using a PANalytical X'Pert Pro HTS diffractometer with a slit of 0.04° at a scanning rate of 9° min^{-1} in the range 4–90°2θ using a Cu-Kα radiation (λ = 1.54 Å).

The ATR-FTIR spectra were recorded using an HTS-XT Bruker Tensor 27 (Bruker, USA) in the range 6000–400 cm^{-1} (resolution 4 cm^{-1}) and 32 interferograms were recorded for each sample.

Surface areas were determined by multipoint N_2 adsorption at 77 K using Quantachrome Quadrasorb instrument. Samples were degassed under vacuum at 120 °C for 1 h prior to analysis. The data were treated in accordance with the BET method.

2.4. Catalyst testing

Typically, the catalyst testing was performed in 16 mL glass vials at room temperature. Glucose solutions at different concentration were prepared by solubilizing the substrate in a 50/50 v/v MeCN/H_2O solution. Subsequently, an appropriate amount of catalyst (14 mg) was added to the solution. The reactions were performed at different reaction times, and samples were taken every 30 min in the first 2 h and at the end of the reaction. Gas sampling studies were conducted on septum sealed vials.

The photocatalytic reactions were performed using three different systems: a Luzchem Photoreactor (Mod. LZC-4, Luzchem Research Inc. ON, CAN) equipped with 14 (8 W each) UVA lamps for a total power of 112 W. The temperature was kept constant at 25 °C for all the reactions. The second system was a 300 W Xenon Oriel Lamp (Mod. 6258, Newport, UK) controlled by a power supply (Mod.69911, Newport, UK). The third lamp used was a 1000 W Xenon Oriel Arc Lamp (Mod.6271, Newport, UK) controlled by a digital power supply (Mod.69920, Newport, UK). Both lamps were equipped with UV filters with a cut-off value of 420 nm (Mod.FSQ-GG420, Newport, UK. Additionally, due to the intense irradiation energy of the lamps, liquid IR filters were installed (Mod.61945 and Mod. 6123NS for the 300 W and 1000 W respectively) to prevent the reaction mixture from overheating. The vials were kept under magnetic stirring and at a constant distance (0.014 m) from the light source for all experiments (Additional Information: Supplementary information Figs. S1–S6).

The glucose conversion and the selectivity towards the partially oxidised products were calculated using the following formulas:

$$\text{Glucose conversion}(\%) = ([Glu]in\text{-}[Glu]out/[Glu]in)$$

$$\text{Gluconic acid selectivity}(\%) = ([Gluconic acid]out/([Gluconic acid]out$$
$$+ [Arabinose]out + [Erythrose + Glyceraldehyde]out$$
$$+ [Formic acid]out))$$

Selectivity values are calculated on a molar basis.

2.5. Product analysis

The glucose stock solutions and reaction products were analysed with a 1200 HPLC Agilent (Agilent, USA) system equipped with a photodiode array detector (DAD) and a refractive index detector (RID). The analytical column used was an Aminex HPX-87H (300 mm × 7.8 mm), 9 μm particle size (Bio-Rad CA, USA) kept at 65 °C and using a 0.025 M H_2SO_4 as eluent with a flow rate of 0.65 mL min^{-1}. The products concentration and glucose conversion were determined using calibration curves. The accurate mass of the oxidised products obtained from glucose was analysed with an Agilent 6510 Q-TOF LC/MS system and interpreted using Agilent MassHunter Workstation Software (Version B.06.00). The column used for the mass spectrometry analysis was a Varian MetaCarb 67H (300 mm × 6.5 mm) (Agilent, USA) kept at 65 °C using a 0.1% w/w formic acid aqueous solution at a flow rate of 0.8 mL min^{-1}. The Q-TOF was operated in positive ESI mode. Hydrogen was detected using, and Agilent 7890 B fitted with pulse discharge ionization detector and calibrated using a standard gas mix. The pressure rise in the sealed vessel due to gas evolution was considered to be negligible.

3. Results and discussion

3.1. Catalytic activity of TiO_2 under visible and UVA light and substrate concentration effect

Fig. 1 shows the time on line plots of conversions obtained with TiO_2 under both visible and UVA light. We were initially surprised to observe conversion and even glucose photo-oxidation under visible light with unmodified TiO_2. Furthermore, by the end of the reaction time at 240 min, conversion under visible light was surprisingly higher than under UVA when 2.8 mM of glucose was used
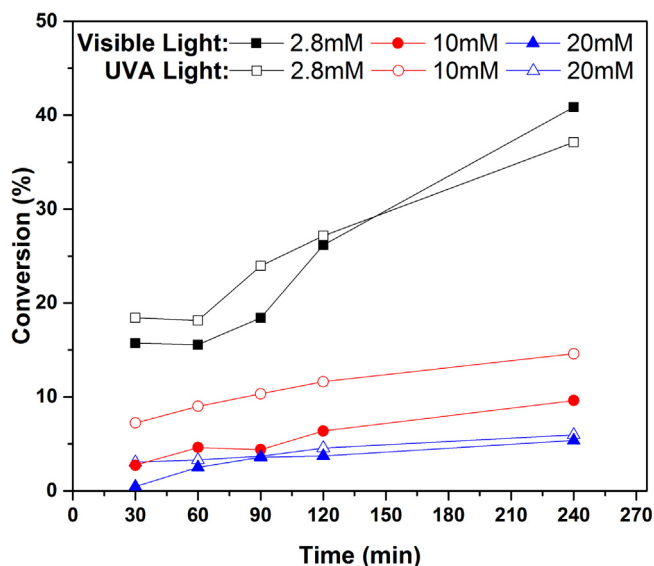
Fig. 1. Glucose conversion under visible and UVA light over 240 min.

Fig. 2. Two possible configurations of the TiO$_2$-glucose complex (Adapted from Kim et al) [25].

as substrate. At the lowest glucose concentration of 2.8 mM, the glucose conversion is 37% after 240 min under UVA light whilst under visible light the final conversion is higher at 42%. We then decided to keep the concentration of the catalyst constant (1 g L^{-1}) while the glucose concentration was increased from 2.8 to 20 mM. For both sets of tests carried out under visible or UVA light, conversion decreases with substrate concentration as expected. For reactions performed with the initial glucose concentration of 10 mM, UVA light proved substantially more effective, whereas higher concentrations result in similar conversions for both types of irradiation.

The mass balances (MB) reported in Table 1 give us an indication of unidentified products, typically as a consequence of mineralization. Again, some interesting and unexpected differences arise by comparing the catalyst performance under UVA and visible light. Firstly, one must acknowledge that under UVA irradiation, the mass balance follows a trend in agreement with conversion; the higher the conversion, the lower the mass balance, suggesting that a mineralization pathway operates. However, the new found activity under visible light does not correlate in the same way with this mineralization pathway and indicates that for the same level of photo-conversion there is little mineralization (see Fig. S7 in Supplementary information). For example, after 240 min of reaction with an initial glucose concentration of 2.8 mM, we obtained 42% conversion and a mass balance of 90% when irradiating with visible light; whereas under UVA light, the mass balance was as low as 81% with a lower glucose conversion of 37%. Interestingly, even when the incident irradiation is not sufficient to promote electrons in the TiO$_2$ conduction band, glucose can still be mineralized. On the other hand, for the reactions run with a glucose concentration of 10 mM, the mass balance displays +99% values under visible light, whereas under UVA light mineralization still plays a significant role as the mass balance equals 96%.

Inspection of Table 1 suggests that by increasing the substrate concentration, gluconic acid selectivity increases from 7 to 12% under visible light and from 0 to 7% under UVA light. Such a trend is the direct consequence of decreasing conversion values. What is more interesting is that the catalyst is clearly more selective towards gluconic acid when irradiated with visible light, suggesting that the selective photo-oxidation route is enhanced under these conditions (see Fig. S9 in Supplementary information). It is therefore clear from our experiments, how it is possible to impart a certain level of selectivity to the overall process by altering the irradiation source even when using the same catalyst.
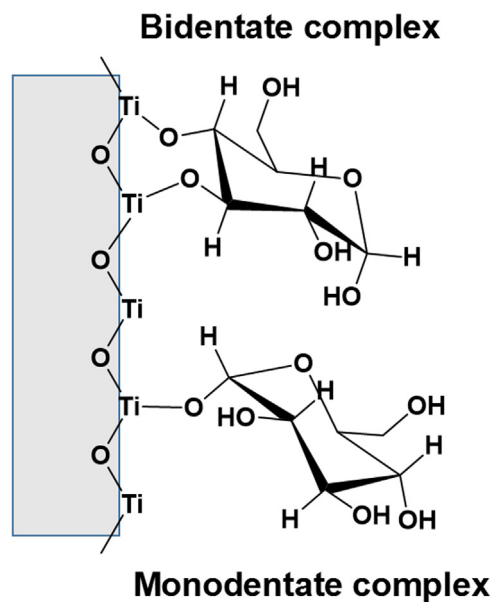
The unexpected photocatalytic activity of TiO$_2$ when irradiated with visible light, and the overall trend in the effect of substrate concentration can be explained by considering the formation of the TiO$_2$-glucose LMCT complex (Fig. 2) identified in 2015 by Kim et al. [25] The formation of this complex is responsible for the visible light absorption ability of the TiO$_2$ via transfer of a photo-excited electron from the highest occupied molecular orbital (HOMO) of glucose to the conduction band of the TiO$_2$. Given this, one can expect that there will be an optimum concentration of such species on the catalyst surface and that above such concentration there would be an oversaturation of adsorption sites and reaction rates will decrease. This is in agreement with the marked reduction in activity for initial concentrations of glucose of 10 mM which is significantly greater than that observed for UVA irradiation (Fig. 1). In Table 1 we have calculated the specific activities (calculated after 240 min on line) for the reactions above, and it is clear that under visible light, the number of millimoles converted by the catalyst is constant at around 18–21 mmol g^{-1}h^{-1} and so appears fairly independent from the concentration of the substrate. The same is observed under UVA light, obtaining specific activities between 18 and 21 mmol g^{-1}h^{-1} for glucose concentrations from 2.8 to 20 mM. It is therefore apparent that under these conditions and in the range of concentrations considered in this study, we are not under diffusion limitation conditions.

3.2. Effect of the TiO$_2$ crystalline structure

In this set of experiments rutile, anatase and P25 were used to assess their respective catalytic activity for selective glucose photo-oxidation. Given our previous results, we decided to carry out these experiments at a low catalyst to substrate ratios and shorter times (120 min) aiming towards better selectivities. All reactions were performed with a catalyst concentration of 1 g L^{-1} and a 20 mM glucose stock solution, and the results are shown in Table 2.

Clearly, in all instances, P25 displayed superior activity to rutile, anatase and the physical mixture of these two. Under visible irradiation, P25 outperforms both rutile and anatase displaying a glucose conversion of 3.7% against 1.7%, and 0.7% respectively. Interestingly, in the experiments performed under visible light irradiation, gluconic acid could not be detected when the pure crystalline phases were used, whereas P25 and the physical mixture of rutile and

Table 1
Glucose photocatalytic conversion with TiO_2 under visible and UVA light after 240 min reaction and glucose concentrations of 2.8, 10 and 20 mM.

Glucose Concentration (mM)	Light source	Conv. (%)	Gluconic Acid Selectivity (%)	C_2–C_5 Aldoses (%)	Specific Activity (mmol g^{-1} h^{-1})	Mass Balance (%)
2.8	visible	42	7	93	21	90
10	visible	10	10	90	18	100
20	visible	5	12	88	19	100
2.8	UVA	37	0	100	18	81
10	UVA	15	6	94	21	96
20	UVA	6	7	93	22	99

Reaction conditions: 240 min reaction, 14 mg of catalyst (1 g L^{-1}).

anatase show 17–18% selectivity to the acid intermediate. This is surprising, particularly considering that in the previous section we showed that higher conversions (associated with lower starting material concentration) were typically associated with lower selectivity to gluconic acid.

Under UVA irradiation, however, gluconic acid is produced by all the studied TiO_2 catalysts. Rutile proved to have higher photoactivity than anatase, with comparable performances to P25 under UVA irradiation, displaying a glucose conversion of 4.3% compared to 4.6% for the P25, whilst anatase displayed only 2% after 120 min of irradiation. On the other hand, anatase under UVA irradiation displayed much higher gluconic acid selectivity (24%) if compared with P25 (10%) and rutile (8%), although this again might be related to the lower level of conversion displayed by anatase (Table 2). Our work indicates that despite rutile's lower surface area it is indeed superior to anatase in the selective photo-oxidation of glucose and that the choice of the TiO_2 allotropic structure also has an effect on the product distribution.

As P25 was the most active catalyst, we decided to also evaluate the effect of mixing the two crystalline phases, rutile, and anatase in a proportion 1:3 (to mimic the typical composition of P25). Under visible light irradiation, the 1:3 physical mixture of rutile and anatase achieved 1.1% glucose conversion, which suggests that some synergy exists when mixing these two phases; however, this level of conversion, is still three times lower than that observed for P25. Interestingly, under visible light, none of the pure TiO_2 phases show gluconic acid in their product distribution; whereas both the physical mixture and P25 show 17–18% selectivity to gluconic acid. There are several examples in the literature on the superior activity of P25 due to the synergic effect of the presence of both rutile and anatase phases in the same solid [26–28]. In fact, the presence of rutile and anatase along with minor amorphous content (generally lower than 5%), forms a heterojunction between the two phases, and the difference in the bandgap position and the presence of an interface, can enhance the separation of the electron-hole pair formed during the process and, at the same time, reduce the recombination rate, thus making the reactive species available for longer. [29–33]

Hurum et al. [28] reported that the superior activity of the TiO_2-P25 is due to several factors such as: the smaller rutile bandgap which extends the range of suitable excitation wavelengths; the stabilisation of the charge separation due to electron transfer from rutile to anatase, and lastly, the small rutile crystallite size which favours this electron-transfer process, creating hot-spots at the interface between the two phases. It is also emphasised that the interface between the rutile particles and anatase in the TiO_2-P25 matrix plays a crucial role in enhancing the catalytic activity, thus explaining why the physical mixture test resulted in an increased glucose conversion, but not to the same extent as that seen with TiO_2-P25. Ohno et al. [26,29] investigated the effect of different TiO_2 physical mixtures in the conversion of naphthalene and related the enhanced activity over anatase and rutile mixtures to the band gap difference of 0.2 eV. This difference can result in the accumulation of charge on the rutile phase as a result of the effective hole scavenging nature of the naphthalene substrate. Given that carbohydrates are equally effective hole-scavengers a similar mechanism is envisaged whereby the accumulated electron charge on the rutile crystallite leads to an upward bending of the conduction band or a thermally activated electron transfer to the anatase [34,35].

It is remarkable that the two crystalline phases, the physical mixture, and the P25 are active at wavelengths greater than 420 nm. This is surprising as in this range the incident photons do not have sufficient energy to promote the electrons in the TiO_2 conduction band. We believe that this activity is the result of the formation of a photoactive ligand to metal charge transfer (LMCT) TiO_2-glucose complex. When glucose is adsorbed on the catalyst surface, the colour change from the typical white to a yellowish tint is in good agreement as reported by Kim et al. [25]. In fact, the formation of this complex is also responsible for the changes in the refractive index of the support (Supplementary information Fig. S10). The peak observed between 480 and 650 nm is due to the formation of the LMCT complex. It can also be seen how under UVA light, due to the formation of highly reactive radical species, the complex formation is hindered and no peak can be observed between 480 and 650 nm. This TiO_2-glucose complex has proven effective in the reduction of metal ions in solution, as the organometallic complex can inject electrons directly in the conduction band of the TiO_2 thus making them available for further reactions.

Table 2
Effect of the different TiO_2 crystalline structures on the product selectivity, product concentrations and total mass balance for the reactions run under visible light and UVA light.

Catalyst	Light source	Conv. (%)	Gluconic Acid (%)	Arabinose (%)	Erythrose + Glycerldehyde (%)	Formic Acid (%)	Specific Activity (mmol g^{-1} h^{-1})
Rutile	visible	1.7	0	32	33	35	12
Anatase.	visible	0.1	0	50	51	0	1
P25	visible	3.7	15	23	14	48	27
Phys Mix	visible	1.1	17	25	21	37	8
Rutile	UVA	4.3	7	27	26	40	31
Anatase	UVA	2	10	29	10	41	14
P25	UVA	4.6	9	43	15	22	33
Phys Mix	UVA	3.0	10	29	14	46	21

Reaction conditions: 120 min reaction, 14 mg of catalyst (1 g L^{-1}). All test resulted in carbon mass balances between 99 and 101%.

Table 3
Effect of the calcination temperature on the P25 on the products selectivity, products concentrations and total mass balance for the reactions run under UVA and visible light.

Catalyst	Light Source	Conv. (%)	Gluconic Acid (%)	Arabinose (%)	Erythrose + Glyceraldehyde (%)	Formic Acid (%)	Specific Activity (mmol g^{-1} h^{-1})
P25	visible	3.7	15	23	14	48	27
P25-500°C	visible	4.5	12	26	20	43	33
P25-600°C	visible	5	13	33	20	34	37
P25	UVA	4.6	9	43	15	33	33
P25-500°C	UVA	6.3	7	44	12	37	45
P25-600°C	UVA	9	7	41	12	39	69

Reaction conditions: 120 min reaction, 14 mg of catalyst (1 g L^{-1}). All test resulted in carbon mass balances between 98 and 100%.
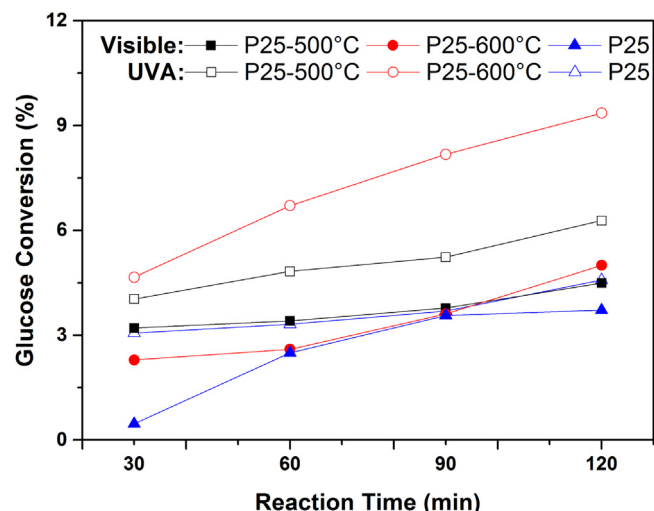
Table 4
Effect of multiple reuses on activity, product selectivity and mass balances over P25–600 °C under visible light and UVA.

Run number	Light Source	Conv. (%)	Gluconic Acid (%)	Arabinose (%)	Erythrose + Glycerldehyde (%)	Formic Acid (%)	Specific Activity (mmol g^{-1} h^{-1})
1st use	visible	5.0	13	33	20	34	37
2nd use	visible	3.0	12	28	17	43	18
3rd use	visible	0.9	14	26	18	43	12
1st use	UVA	9.0	7	41	12	39	69
2nd use	UVA	7.7	7	41	14	38	60
3rd use	UVA	6.5	6	43	11	40	45

Reaction conditions: 120 min reaction, 14 mg of catalyst (1 g L^{-1}). All test resulted in mass balances between 99 and 102%.
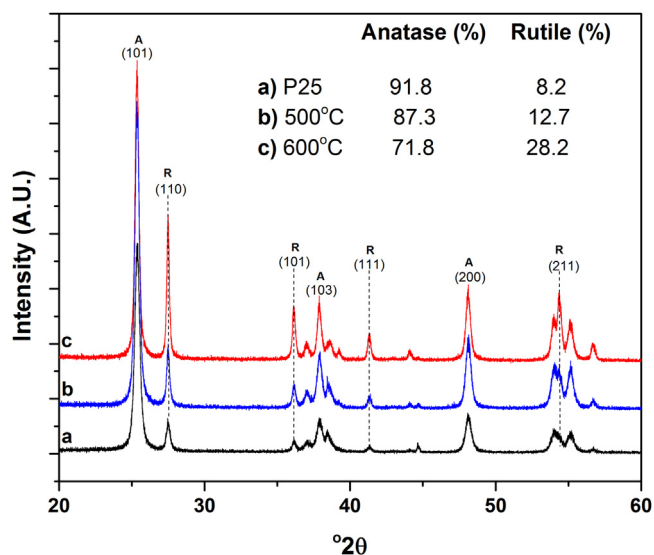
Fig. 3. XRD pattern for a) TiO$_2$-P25, b) P25–500 °C and b) P25–600 °C. Inset: The relative concentrations of the anatase and rutile determined by Rietveld refinement excluding amorphous content.

Fig. 4. Glucose conversion obtained after heat treatments of P25 at different temperatures.

3.3. Effect of the calcination temperature

In the previous section, we conclude that there is a synergistic effect when mixing rutile with anatase, but the effect is much greater in P25. We also found that rutile was more active than anatase. In view of this, we decided to modify the crystalline composition of P25 by thermal treatment aiming to increase the content of rutile and therefore, the photocatalytic activity. As shown in Fig. 3 and in Table 3, increasing the temperature during the heat treatment process results in higher rutile content. In fact, the UV–Vis absorption profile shifts to higher wavelengths (Supplementary information Fig. S11-12). Surface area analysis showed the expected decrease from 48 m^2 g^{-1} for the P25 to 43 and 32 m^2 g^{-1} for the 500 and 600 °C calcined catalyst respectively consistent with the increase in rutile content and phase crystallinity. X-ray powder diffraction (XRD) indicates that the rutile content increased from 8.2% in the untreated P25 to 28.2% for the sample treated at 600 °C (Fig. 3). The treated P25 powders namely, P25–500 °C and P25–600 °C were tested and their catalytic activity vs. time on line up to 120 min is displayed in Fig. 4. Clearly, the materials

with higher rutile content (P25–600 °C) displayed higher catalytic activity with a glucose conversion of 9% under UVA light compared with 4.6% for the untreated P25 (Fig. 4, Table 3). This is expected based upon the earlier studies on the activity of the pure phases; the increased rutile content directly affects the activity of the catalyst incrementing its turnover frequency under UVA light without modifying the product distribution. In fact, the calcination process increases the percentage of rutile crystallites in the TiO$_2$-P25 matrix, and therefore, the number of interfaces between the two phases which is responsible for the electron-transfer and the charge separation mechanisms necessary to guarantee long-lived and available radical species. Interestingly, under visible light, there were no substantial differences in the performances of the two materials with regards to both activity and selectivity (Table 4).

3.4. Reaction pathway and recycling studies

The photo-conversion of glucose to partial oxidation products has been reported using supported metal nanoparticles on TiO$_2$ under several illumination sources. The results obtained in this work as displayed in Table 4, support the initial findings of Colmenares et al. [21] and Chong et al. [19]. In fact, we were able

to determine and quantify the presence of partial oxidation products coming from the two distinct reaction pathways described in the literature, which included gluconic acid, arabinose, a mixture of erythrose and glyceraldehyde and formic acid. The presence of gluconic acid could not be related to Chong's experimental results (Supplementary information Scheme S1) in which the presence of formic acid and other oxidation products is explained due to the loss of H_2 and HCOOH during the photocatalytic process. On the other hand Colmenares' work showcases the production of gluconic and glucaric acid albeit under pure UV irradiation. From our time on line data (Supplementary information Figs. S8-10-13), it is possible to appreciate that the product distribution profiles are very similar across all reactions. In fact, in all cases, the dominant products were arabinose and formic acid with combined selectivity >80% of the oxidation products. Interestingly, by taking a closer look, we can see that arabinose is rapidly formed after 30 min of reactions along with formic acid, with traces of gluconic acid which become more significant after 60 min of reaction. This suggests that the rate of H_2 and HCOOH evolution is higher than the glucose oxidation to gluconic acid. The formation of erythrose (C_4) and glyceraldehyde (C_3) is in good agreement with the decrease in the arabinose selectivity, thus suggesting a sequential reaction. The reaction pathway described involves multiple parallel and subsequent reactions which involve the presence of several partial oxidation products. To maximise the selectivity of the process towards the production of gluconic acid, and avoid the competitive loss of H_2 and HCOOH with the production of arabinose, probably a batch-like configuration is not the ideal reactor set-up. Better results could probably be obtained by using a flow-type reactor with a supported catalyst to minimise the contact time between of the substrate, or by using TiO_2-supported metal nanoparticles which have shown to be able to impart some level of selectivity in photo-oxidation reactions [36–39]. Interestingly, over multiple reuses of the best performing material (TiO_2–600 °C) under UVA and visible light, a decrease in activity was observed with glucose conversion values dropping from 9% to 6.5% under UVA light and 5% to 0.9 under visible light. The catalyst activity dropped with no significant changes in the product distribution values, indicating a loss of active sites on the TiO_2 surface for reasons currently under study. Clearly, to make this process feasible for industrial applications, the catalyst stability and reusability upon multiple runs are crucial parameters that will need careful tuning and optimisation.

3.5. Effect of the lamp power and filters

We decided to utilise two Xenon lamps of 300 W and 1000 W under the same experimental conditions to assess the effect of the light intensity on glucose conversion (Supplementary information Table S1, Fig. S14–15). Initially, the two systems were tested using P25 as a catalyst and a 20 mM glucose solution in a 50/50 MeCN/H_2O. The catalytic results with both irradiation sources and the effect of visible light filters are displayed in Fig. 5. Firstly, there is a clear effect of the power utilised and, with the 1000 W lamp, we obtained 23% conversion after 120 min while only 14% was obtained with the 300 W lamp. The visible light filters do result in a dramatic decrease in conversion, but surprisingly, it is the 300 W lamp that produced higher conversion: conversion dropped to 1.7% and 3.7% for the 1000 W and 300 W respectively (Fig. 5).

These results clearly show that the power of the light sources has to be chosen according to the experimental set-up used. In fact, more irradiance does not necessarily imply better results (Supplementary information Fig. S14–15). Lower power lamps also have benefits as the arc sources are smaller and, in some cases, even brighter than the more powerful lamps, consequently, it is possible to achieve high flux densities on small targets using small lamps. It is also worth considering that smaller lamps are easier to operate as
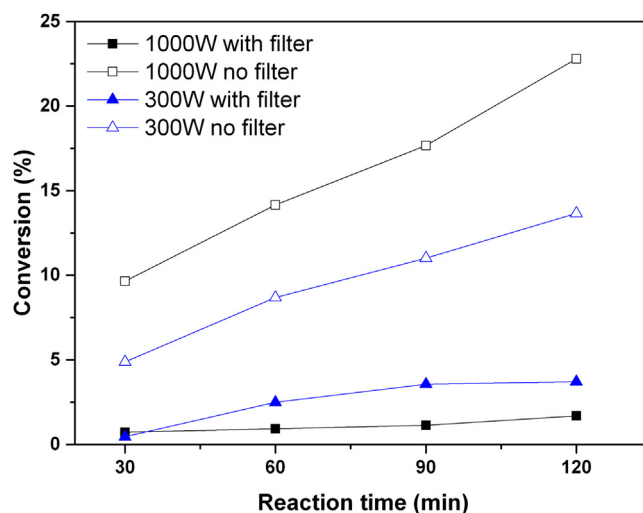

Fig. 5. Glucose conversion obtained using two different Xenon lamps (300, and 1000 W respectively) with and without the visible light filter using the 50/50 v/v MeCN/H_2O mixture.

they do not require additional filters to dissipate the heat produced and hence avoid thermal variations and heating of the reaction mixture. Therefore, the application of every lamp is really reaction and configuration sensitive and the choice of which configuration to use has to be made carefully. Additionally, when photocatalytic results are reported, information on the lamp hours and the average lifetime of the irradiating source should also be available, as the performances of the same lamp throughout its life cycle can vary dramatically (Supplementary information Table S3). To further corroborate the importance of choosing the right light source for a specific application, a reaction with the TiO_2–600 °C was performed under natural light for 7 h and the results are reported in the Supplementary information Table S4. The light intensity measured at the beginning of the reaction (10 am) was found to be 6000 lx which for sunlight irradiation, assuming the relationship of 0.0079 W m^{-2} per lx is equal to 47.4 W m^{-2}, a value 100 times smaller than the one recorded for the 300 W Xenon lamp with the 420 nm filter installed. This low irradiation level is typical for a cloudy day in Liverpool, however, despite these low-light-intensity conditions (Supplementary information Fig. S14), we observed 3.2% glucose conversion with a 15% selectivity towards gluconic acid.

3.6. Effect of the solvent: experiments in pure water

Arguably, water would be the preferred solvent to carry out the photocatalytic oxidation as it offers a number of practical advantages, but also because it is the choice for conventional catalytic studies for glucose oxidation [2]. When pure H_2O was used as reaction medium, the conversion values dropped to 9.5% (1000 W) and 6.4% (300 W) without filters, and to around 2% with the filters installed (Fig. 6). The significant differences in the conversion values can be explained by taking into account the different activity of the support under those conditions. Generally, UV light filters are identified by their cut-off value which is defined as 50% transmittance of the radiation at the nominal wavelength. This value clearly implies a certain degree of transmission of the wavelengths in the range ±20 nm of the nominal value. Therefore, even with the filter installed, it is possible to partially excite the TiO_2 bandgap explaining the apparent activity under visible light in combination with the formation of the LCMT complex. When the filters are removed, the catalyst is exposed to both the UV and visible part of the spectrum and under these circumstances the photons have enough energy to start the photocatalytic process.
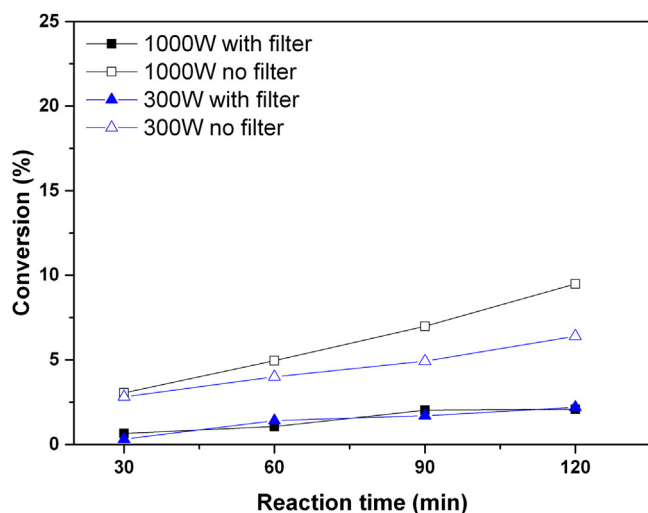
Fig. 6. Glucose conversion obtained using two different Xenon lamps (300, and 1000 W respectively) with and without the visible light filter using pure H_2O as a solvent.

The solvent choice has an impact on the substrate conversion in photochemical reactions. Despite it not being an ideal green solvent acetonitrile is suitable because it has no absorption in either the ultraviolet or visible region of the spectrum, it is a polar and aprotic solvent, and has very little chemical reactivity.

In the literature, there are some examples of H_2O/MeCN mixtures in photochemical applications, but the role of the MeCN is not yet fully understood because of the complexity of the chemistry involved [17,36,40]. Redmond and Fitzmaurice proved that the TiO_2 flatband potential is affected by non-aqueous solvents, and they reported that in the absence of the proton adsorption-desorption mechanism negative values were observed in MeCN, EtOH, and MeOH, whereas when electrolytes and water are added to the systems, significant positive shifts were observed [41]. Therefore, when considering a photocatalytic system, it is necessary to consider the effect of the solvents on the zero-point charge value of the material surface given that the adsorbed species along with the effect of the solvent might dramatically affect the photo-activity of the material.

Additionally, various authors suggested that the lifetime of singlet oxygen ($^1O_2$) species produced during the photochemical process might be increased when aprotic, and polar solvents are present in the solution [42]. Therefore, the longer lifetime of radical species in MeCN compared to pure water would explain the differing catalytic activity in various reaction media, but the determination and quantification of these reactive radicals exceeds the purpose of this work.

4. Conclusions

In this work we have shown how TiO_2 is an active photocatalyst under visible light for the transformation of glucose to a range of oxidation products. Furthermore, under visible light, titania was more selective to gluconic acid with less mineralization to CO_2 as compared to UVA light. This visible light photo-activity over unmodified titania was achieved through the exploitation of a glucose-TiO_2 charge transfer complex whereby a metal-organic complex is formed with the reactant. This demonstrates the crucial role of the adsorption-desorption mechanisms in photocatalytic reactions which are sometimes overlooked. The crystalline structure of TiO_2 determines the activity and extent of glucose conversion, with P25 being more active than rutile or anatase. Furthermore, calcination of P25 at 500 and 600 °C resulted in improved activity due to the increased rutile content. The role of the solvent was evaluated and despite all the positive effects that the addition of MeCN has on the glucose conversion and the enhancement of the catalytic activity, it is not a green solvent, and it is desirable to substitute it with a solvent that is less toxic while remaining chemically stable during the photocatalytic process or else design more efficient catalysts able to produce selective reactions in pure water. Furthermore, despite the low irradiation intensity, titania was also active towards the same reaction products when exposed to natural sunlight on a cloudy day in Liverpool (UK) suggesting that the opportunity of using natural sunlight is indeed an attractive one. We believe that the insights gained from this work can be extended to the photocatalytic conversion of other carbohydrate and polysaccharide substrates readily available from biomass, where the formation of analogous surface complexes might also confer visible light activity.

Appendix A. Supplementary data

Supplementary data associated with this article can be found, in the online version, at http://dx.doi.org/10.1016/j.apcatb.2016.08.035.

References

[1] S. Biella, L. Prati, M. Rossi, Selective oxidation of D-glucose on gold catalyst, J. Catal. 206 (2002) 242–247.
[2] N. Dimitratos, J.A. Lopez-Sanchez, G.J. Hutchings, Selective liquid phase oxidation with supported metal nanoparticles, Chem. Sci. 3 (2012) 20–44.
[3] M. Comotti, C. Della Pina, E. Falletta, M. Rossi, Is the biochemical route always advantageous? The case of glucose oxidation, J. Catal. 244 (2006) 122–125.
[4] T. Mallat, A. Baiker, Oxidation of alcohols with molecular oxygen on solid catalysts, Chem. Rev. 104 (2004) 3037–3058.
[5] I. Nikov, K. Paev, Palladium on alumina catalyst for glucose oxidation: reaction kinetics and catalyst deactivation, Catal. Today 24 (1995) 41–47.
[6] S.H.O.S.F. SHIGEO, Process for producing gluconic acid., EP0142725 (A1), (1985).
[7] C.D. Pina, E. Falletta, M. Rossi, Update on selective oxidation using gold, Chem. Soc. Rev. 41 (2012) 350–369.
[8] H. Zhang, N. Toshima, Glucose oxidation using Au-containing bimetallic and trimetallic nanoparticles, Catal. Sci. Technol. 3 (2013) 268–278.
[9] G. Wu, T. Chen, G. Zhou, X. Zong, C. Li, H2 production with low CO selectivity from photocatalytic reforming of glucose on metal/TiO2 catalysts, Sci. China Ser. B-Chem. 51 (2008) 97–100.
[10] P. Gomathisankar, D. Yamamoto, H. Katsumata, T. Suzuki, S. Kaneco, Photocatalytic hydrogen production with aid of simultaneous metal deposition using titanium dioxide from aqueous glucose solution, Int. J. Hydrogen Energy 38 (2013) 5517–5524.
[11] L. Zhang, J. Shi, M. Liu, D. Jing, L. Guo, Photocatalytic reforming of glucose under visible light over morphology controlled Cu2O: efficient charge separation by crystal facet engineering, Chem. Commun. 50 (2014) 192–194.
[12] J.C. Colmenares, A. Magdziarz, M.A. Aramendia, A. Marinas, J.M. Marinas, F.J. Urbano, J.A. Navio, Influence of the strong metal support interaction effect (SMSI) of Pt/TiO2 and Pd/TiO2 systems in the photocatalytic biohydrogen production from glucose solution, Catal. Commun. 16 (2011) 1–6.
[13] M. Bellardita, E.I. García-López, G. Marcì, L. Palmisano, Photocatalytic formation of H2 and value-added chemicals in aqueous glucose (Pt)-TiO2 suspension, Int. J. Hydrogen Energy 41 (2016) 5934–5947.
[14] B. Zhou, J. Song, T. Wu, H. Liu, C. Xie, G. Yang, B. Han, Simultaneous and selective transformation of glucose to arabinose and nitrosobenzene to azoxybenzene driven by visible-light, Green Chem. (2016).

[15] B. Zhou, J. Song, H. Zhou, T. Wu, B. Han, Using the hydrogen and oxygen in water directly for hydrogenation reactions and glucose oxidation by photocatalysis, Chem. Sci. 7 (2015) 463–468.

[16] J.C. Colmenares, R. Luque, Heterogeneous photocatalytic nanomaterials: prospects and challenges in selective transformations of biomass-derived compounds, Chem. Soc. Rev. (2014).

[17] J.C. Colmenares, A. Magdziarz, Room temperature versatile conversion of biomass-derived compounds by means of supported TiO_2 photocatalysts, J. Mol. Catal. A: Chem. 366 (2013) 156–162.

[18] M. Bellardita, E.I. Garcia-Lopez, G. Marci, B. Megna, F.R. Pomilla, L. Palmisano, Photocatalytic conversion of glucose in aqueous suspensions of heteropolyacid-TiO_2 composites, RSC Adv. 5 (2015) 59037–59047.

[19] R. Chong, J. Li, Y. Ma, B. Zhang, H. Han, C. Li, Selective conversion of aqueous glucose to value-added sugar aldose on TiO_2-based photocatalysts, J. Catal. 314 (2014) 101–108.

[20] J.C. Colmenares, A. Magdziarz, K. Kurzydlowski, J. Grzonka, O. Chernyayeva, D. Lisovytskiy, Low-temperature ultrasound-promoted synthesis of Cr–TiO_2-supported photocatalysts for valorization of glucose and phenol degradation from liquid phase, Appl. Catal. B: Environ. 134–135 (2013) 136–144.

[21] J.C. Colmenares, A. Magdziarz, A. Bielejewska, High-value chemicals obtained from selective photo-oxidation of glucose in the presence of nanostructured titanium photocatalysts, Bioresour. Technol. 102 (2011) 11254–11257.

[22] M. Janus, A.W. Morawski, New method of improving photocatalytic activity of commercial Degussa P25 for azo dyes, decomposition, Appl. Catal. B-Environ. 75 (2007) 118–123.

[23] S. Ahmed, M.G. Rasul, W. Martens, R. Brown, M.A. Hashib, Advances in heterogeneous photocatalytic degradation of phenols and dyes in wastewater: a review, Water Air Soil Pollut. 215 (2011) 3–29.

[24] I. Tacchini, E. Terrado, A. Anson, M.T. Martinez, Preparation of a TiO_2-MoS_2 nanoparticle-based composite by solvothermal method with enhanced photoactivity for the degradation of organic molecules in water under UV light, Micro Nano Lett. IET 6 (2011) 932–936.

[25] G. Kim, S.-H. Lee, W. Choi, Glucose–TiO_2 charge transfer complex-mediated photocatalysis under visible light, Appl. Catal. B: Environ. 162 (2015) 463–469.

[26] T. Ohno, K. Tokieda, S. Higashida, M. Matsumura, Synergism between rutile and anatase TiO_2 particles in photocatalytic oxidation of naphthalene, Appl. Cata. A: Gen. 244 (2003) 383–391.

[27] S. Bakardjieva, J. Šubrt, V. Štengl, M.J. Dianez, M.J. Sayagues, Photoactivity of anatase–rutile TiO2 nanocrystalline mixtures obtained by heat treatment of homogeneously precipitated anatase, Appl. Catal. B: Environ. 58 (2005) 193–202.

[28] D.C. Hurum, A.G. Agrios, K.A. Gray, T. Rajh, M.C. Thurnauer, Explaining the enhanced photocatalytic activity of degussa P25 mixed-phase TiO_2 using EPR, J. Phys. Chem. B 107 (2003) 4545–4549.

[29] T. Ohno, K. Sarukawa, K. Tokieda, M. Matsumura, Morphology of a TiO_2 photocatalyst (Degussa, P-25) consisting of anatase and rutile crystalline phases, J. Catal. 203 (2001) 82–86.

[30] R.I. Bickley, T. Gonzalez-Carreno, J.S. Lees, L. Palmisano, R.J.D. Tilley, A structural investigation of titanium dioxide photocatalysts, J. Solid State Chem. 92 (1991) 178–190.

[31] A. Fujishima, X. Zhang, D.A. Tryk, TiO2 photocatalysis and related surface phenomena, Surf. Sci. Rep. 63 (2008) 515–582.

[32] J. Schneider, M. Matsuoka, M. Takeuchi, J. Zhang, Y. Horiuchi, M. Anpo, D.W. Bahnemann, Understanding TiO2 photocatalysis: mechanisms and materials, Chem. Rev. (2014).

[33] J. Zhang, Q. Xu, Z. Feng, M. Li, C. Li, Importance of the relationship between surface phases and photocatalytic activity of TiO2, Angew. Chem. 120 (2008) 1790–1793.

[34] W.W. Dunn, Y. Aikawa, A.J. Bard, Characterization of particulate titanium dioxide photocatalysts by photoelectrophoretic and electrochemical measurements, J. Am. Chem. Soc. 103 (1981) 3456–3459.

[35] R. Morelli, S. Russo-Volpe, N. Bruno, R. Lo Scalzo, Fenton-dependent damage to carbohydrates: free radical scavenging activity of some simple sugars, J. Agric. Food Chem. 51 (2003) 7418–7425.

[36] J.C. Colmenares, A. Magdziarz, O. Chernyayeva, D. Lisovytskiy, K. Kurzydłowski, J. Grzonka, Sonication-assisted low-temperature routes for the synthesis of supported Fe–TiO2 econanomaterials: partial photooxidation of glucose and phenol aqueous degradation, ChemCatChem 5 (2013) 2270–2277.

[37] D. Spasiano, L. del Pilar Prieto Rodriguez, J.C. Olleros, S. Malato, R. Marotta, R. Andreozzi, TiO2/Cu(II) photocatalytic production of benzaldehyde from benzyl alcohol in solar pilot plant reactor, Appl. Catal. B: Environ. 136–137 (2013) 56–63.

[38] A. Lüken, M. Muhler, J. Strunk, On the role of gold nanoparticles in the selective photooxidation of 2-propanol over Au/TiO2, Phys. Chem. Chem. Phys. 17 (2015) 10391–10397.

[39] S. Linic, U. Aslam, C. Boerigter, M. Morabito, Photochemical transformations on plasmonic metal nanoparticles, Nat. Mater. 14 (2015) 567–576.

[40] Y. Shiraishi, T. Hirai, Selective organic transformations on titanium oxide-based photocatalysts, J. Photochem. Photobiol. C: Photochem. Rev. 9 (2008) 157–170.

[41] G. Redmond, D. Fitzmaurice, Spectroscopic determination of flatband potentials for polycrystalline titania electrodes in nonaqueous solvents, J. Phys. Chem. 97 (1993) 1426–1430.

[42] Y.F. Huang, M. Zhang, L.B. Zhao, J.M. Feng, D.Y. Wu, B. Ren, Z.Q. Tian, Activation of oxygen on gold and silver nanoparticles assisted by surface plasmon resonances**, Angew. Chem.-Int. Ed. 53 (2014) 2353–2357.